Research Article

Mediterranean Marine Science
Indexed in WoS (Web of Science, ISI Thomson) and SCOPUS
The journal is available on line at http://www.medit-mar-sc.net
DOI: http://dx.doi.org/10.12681/mms.22462

The contribution of wind-wave energy at sea bottom to the modelling of rhodolith beds distribution in an off-shore continental shelf

Sabrina AGNESI, Aldo ANNUNZIATELLIS, Roberto INGHILESI, Giulia MO and Arianna ORASI

Italian National Institute for Environmental Protection and Research, Via Vitaliano Brancati 60, 00144, Rome, Italy

Corresponding author: sabrina.agnesi@isprambiente.it

Handling Editor: Stelios SOMARAKIS

Received: 21 February 2020; Accepted: 15 May 2020; Published on line: 3 July 2020

Abstract

The study aims to investigate the relationship between the presence of rhodolith beds and the effect on the shelf bottom boundary layer due to the action of surface wind waves. The study area is situated off-shore and north-west of Elba Island in the Western Mediterranean Sea, an area known to be characterized by rhodolith beds. A binomial logistic regression model is used in order to analyse the relationship between wind-wave energy at sea bottom, bathymetry and rhodolith bed occurrence. The results indicate a positive correlation between rhodolith bed occurrence and wave energy, while the relation with bathymetry is weaker in all the trials. The wave energy confidence interval associated to the rhodolith bed probability is also estimated, thereby informing on wind wave energy values required for the modelling of this particular benthic habitat in off-shore shelf areas.

Keywords: Broad scale habitat map (BSHM); wave energy; rhodolith bed; Mediterranean Sea; continental shelf.

Introduction

The availability of spatial data on the distribution of species and habitats is a crucial aspect for the implementation of marine policies requiring marine spatial planning, management and conservation. In such contexts, geo-referenced information on species and habitat distribution is used for the assessment of ecological / conservation status of the biological features. Biological spatial information can also be used in analysis processes involving the management of human impacting activities that require spatial planning measures considered crucial for nature conservation (Cogan *et al.*, 2009; Korpinen *et al.*, 2013; Galparsoro *et al.*, 2014; Levin *et al.*, 2014; Agnesi *et al.*, 2017; Andersen *et al.*, 2018). In light of the sparse availability of pan-European spatial data on marine species and habitat distribution, several European funded projects have focused, over the course of the last decades, on delivering national, transnational and pan-European broad scale seabed habitat maps (BSHMs) (Connor *et al.*, 2006; Al-Hamdani & Reker, 2007; Cameron and Askew, 2011; Vasquez *et al.*, 2015). BSHMs result from models that rely on the use of spatial data describing abiotic variables (e.g. depth, seabed substrate, light, water temperature, salinity, wave energy, etc.) that are known to influence the distribution of seabed habitats and their related assemblages. The advantage of modelled BSHMs is linked to the lower cost of abiotic variable spatial data acquisition and modelling (Roff and Taylor, 2000; Roff *et al.*, 2003) and the potentially wide coverage that can be achieved by merging different existing datasets. On the other hand, the modelling process is limited by the knowledge of abiotic variable threshold values that are biologically relevant for the definition of modelled habitat distributions, and by the resolution of the abiotic variable spatial layers that are required in order to model the distinct habitat distribution.

In this context, bed stress is a physical variable known to influence the distribution of several seabed habitats (Harris, 2012; Rattray *et al.*, 2015). In general, the hydrodynamic stress at the sea bottom is due to several interacting processes related to the action of winds, tides and density differences (Kantha & Clayson, 2000). Wind-wave and tidal motions are important in inner-shelf areas, where they can induce oscillating boundary layers which are relatively thin, generally turbulent, layers imbedded in the larger bottom boundary layer associated with currents (Grant & Masden, 1986). While tides are responsible for producing low-frequency velocity oscillations on many shallow coastal areas, their weakness in most of the Mediterranean implies that shelf circulation in the region is principally wind-dominated (Pugh & Woodworth, 2014).

Wind-waves generated at the sea surface are associated with a complex orbital velocity distribution in the water column beneath. In a relatively shallow sea the

friction due to the water oscillation close to the bottom is a source of turbulent kinetic energy, which is a manifestation of the shear stress. Boundary layer dynamics relate the bed shear stress and the vertical variation of kinetic energy, which is entirely turbulent close to the bottom, and mostly due to the mean velocity system at the external edge of the boundary layer. The dynamics depend clearly on the morphology and the nature of the seabed, the presence of benthic species, the sediment typology and also on the stability of the water column.

The extent of the boundary layer depends on the sea depth and the height of the waves: in inner-shelf areas exposed to the swell produced by an intense storm the wave boundary layer may extend from the bottom up to the sea surface. The knowledge of significant wave height and mean period of the wind waves allows to estimate the orbital velocity close to the bottom, assuming the waves are randomly distributed in a parametric spectrum, the bottom is reasonably flat, the water stratification is neutral and in the absence of sediment. From the orbital velocity near the bottom, the kinetic energy can be calculated (Soulsby, 2006). Alternatively, the wave shear stress may be estimated in a similar way using an empirical wave friction factor (Soulsby, 1997).

Kinetic energy on the sea bottom (due to waves / currents) is one of the environmental factors known to influence the distribution of several coastal and continental shelf Mediterranean benthic assemblages. The infralittoral rocky bottom algal assemblages have a characteristic distribution that reflects the degree of wave energy exposure present in a given area. For this reason, infralittoral algal associations are classified based on the different energy patterns (Templado *et al.*, 2009). In the circalittoral zone, the variation and distribution of different rocky reef assemblages is also influenced by kinetic energy: depending on the amount of energy at sea bottom and the nutrients conveyed, the predominantly faunal composition of the assemblages is composed of different arrays of characteristic species (Michez *et al.*, 2014). Rhodolith beds, composed of free-living coralline red algae, are found on circalittoral soft bottoms. Their distribution is considered dependent on the presence of water motion from bottom currents, waves and tides in mesotrophic and oligotrophic water conditions and within the ecological constraints of light and temperature (Steller and Foster, 1995; Marrack, 1999; Mitchell and Collins, 2004). More specifically, rhodolith beds require moderate current speeds to prevent siltation that would lead to burial of the living thalli, and guarantee sufficient rolling of the thalli in order to prevent their colonisation by bryozoans and other filamentous epiphytes (Birkett *et al.*, 1998; Marrack, 1999). While the rocky infralittoral and circalittoral assemblages described above have small spatial extensions and are difficult to model in a broad scale map, rhodolith beds have a wider extension and can potentially be portrayed in a BSHM provided that adequate modelled spatial data on kinetic energy are available. The latter can be used to define the most appropriate energy on sea bottom thresholds that can be correlated to the habitat's presence.

Several studies have investigated the relationship between energy at sea bottom, due to waves and currents, and the formation and persistence of rhodolith beds. The energy threshold required to induce thalli movement is described by Marrack (1999) while Harris *et al.* (1996) provide a similar description in flume experiments. Recent studies have highlighted the importance of energy as one of the pivotal factors determining the presence and morphology of rhodolith beds (De Falco *et al.*, 2011; Sañé *et al.*, 2016; Joshi *et al.*, 2017). In particular De Falco *et al.* (2011), investigating a morphologically complex domain, found that the spatial distribution of carbonate sedimentary *facies* was mainly influenced by the energy of the currents at the bottom associated with storms rather than by the wave climate at the surface. Sañé *et al.* (2016), considering only indirect measures of the hydrodynamics in their regional factor, did not find any statistical correlation of the 'region' with the morphology, size or growth form of rhodoliths. In particular, the analysis of Joshi *et al.* (2017) was based on coupled hydrodynamics-sediment transport models. They considered both currents and orbital wave velocities at the bottom finding clear evidence of strong interactions among hydraulic energy, maërl grain morphology and sediment mobility. Storm waves were recognised as the dominant driving force for sediment transport, and wave action at the bottom was found to be significantly more important than benthic currents both during calm periods and storms. They demonstrated in their study that the combined wave-current sediment mobility during storm situations was the best physical surrogate and hydrodynamic variable for the distribution of rhodolith beds.

The present study was carried out within the framework of the EMODnet (Phase II 2013-2016) Seabed habitat project. This project produced a pan-European BSHM (250-meter pixel size) representing habitats that could be adequately portrayed in a 250 m /pixel resolution map. The Mediterranean BSHM was modelled based on limited abiotic variables that were available at sufficient resolution for the entire basin (depth, seabed substrate and light). Energy at the seabottom was not used in the model as the resolution of the available spatial data was too coarse (more than 2 km). The present case study, conducted in a test area located in the western Mediterranean, identifies the correlation between wave-induced kinetic energy, through a 250 m energy layer, and rhodolith bed occurrence. In so doing, it defines the wave energy values at the sea bottom that can be used to model rhodolith distribution in future Mediterranean BSHMs.

Materials and Methods

The study area (Fig.1A) is located to the northwest of Elba island in the western Mediterranean and extends over a surface area of about 50 km^2. Bathymetric data, collected during summer 2013 (Agnesi *et al.*, 2015; ISPRA, 2014) in a portion of the study area was integrated with the EMODnet bathymetry spatial layer at a 250 m resolution.

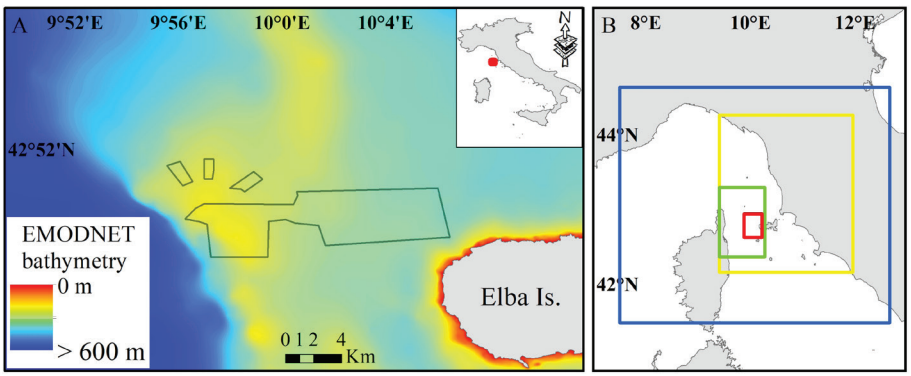

Fig. 1: A) Map of the study area with the indication of the area with high resolution bathymetry (black lines); B) North Tyrrhenian grids: regional resolution (1/60) blue, high resolution (1/120) yellow, very high resolution (1/240) green, target resolution area (1/480) red.

Wave energy at the seabed

The wave climate in the study area was evaluated using the Mediterranean Coastal Wave forecasting system (Mc-Waf). Mc-Waf operates in the Mediterranean Sea using successive levels of nesting of the WAM model (Komen *et al.*, 1994) to simulate the propagation of wind wave energy from the Mediterranean scale to the regional and the costal scale (Inghilesi *et al.*, 2016). In order to simulate the wind waves at the target degree resolution 1/480, a series of nestings were applied to a regional grid of the Tyrrhenian Sea, as shown in Figure 1B with the following level of degree resolution: 1/60, 1/120, 1/240, 1/480. The EMODnet bathymetry data was used at the regional scale, while a mosaic of EMODnet bathymetry and multibeam data was used in the higher resolution and target areas.

The wind forcing was generated using the Bologna Limited Area Model (BOLAM) at 7.2x7.2 km^2 resolution (Casaioli *et al.*, 2014). The wave energy at the seabed was evaluated using the Soulsby and Smallman method (Soulsby, 2006). The method is based on the approximated formula $(U_{rms}\ T_n)/\ H_s = 0.25/(1+At^2)^3$ where U_{rms} is the root-mean-square orbital velocity of the wind waves, T_n is a wave period scale based on the gravity acceleration g and the local depth h, $T_n = (h/g)^{1/2}$. A(t) is a function of the parameter T_n/T_z. Hs and Tz are taken as, respectively, the hourly significant wave height and the hourly mean spectral period of the waves at the surface. The random distribution of the wind waves was assumed parametrized as in the JONSWAP spectrum (Hasselmann *et al.*, 1973).

The distribution of the wind wave kinetic energy at the seabed at the 90-percentile level was calculated in the period October 2012 - March 2015.

Presence/absence of rhodolith beds

The presence of rhodolith beds in this relatively wide area of the mid continental shelf has been described in literature (Agnesi *et al.*, 2015; Bianchi *et al.*, 1996). Rhodolith distribution data was collected in 2013 within the framework of a project funded by the Italian Ministry of Fishery and Agriculture (ISPRA, 2014). Georeferenced videos of the seabed were obtained through ROV transects (red lines in Fig. 2). Image analysis of frame shots

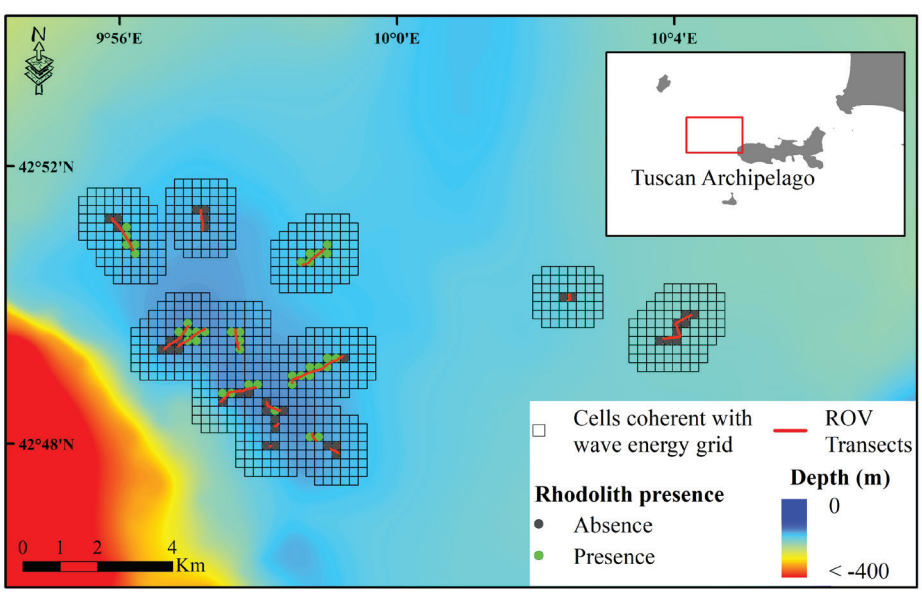

Fig. 2: Distribution of ROV transects and grid cells coherent with the wave energy grid. Dark grey and green points represent the grid sectors characterized by rhodolith bed absence and presence.

extracted from the videos every 10 seconds was used to describe sea bottom characteristics and habitats (Agnesi *et al.*, 2015). The latter results were used to identify sectors of each transect characterized by the presence of rhodolith beds. For the purpose of this work, a rhodolith bed is defined as a condition in which the spatial coverage of the rhodoliths observed in a frameshot extends over >50% of the examined photographic frame area.

An empty vector grid with 250 m x 250 m cells, spatially coherent with the energy layer, was created. A specific spatial dataset of rhodolith bed presence/absence was constructed by intersecting the empty vector grid with the transect sectors containing rhodolith presence/absence information (Fig. 2). The procedure used to assign the rhodolith presence/absence to the grid cells is illustrated in Figure 3. The centroid of the grid cell occurring along each transect is assigned with a unique presence/absence value.

Figure 2 illustrates grid cell rhodolith bed presence/absence assignation according to the above described procedure. Energy values corresponding to each rhodolith bed presence/absence point were extracted for subsequent statistical elaboration.

Data Analysis

A database was constructed as follows:

Y = a binary variable (0/1) indicating the absence/presence of a rhodolith bed;

X_1 = the wave energy value at the seabed (N/m^2);

X_2 = the value of bathymetry (m);

An exploratory data analysis was carried out using R software (R Core Team, 2017). As a preliminary analysis, a Kernel density plot was drawn. The Kernel density estimation is a non-parametric method for estimating the probability density function (PDF) of a continuous random variable. The R function density() was used to obtain the plots.

The Variance Inflation Factors (VIF) value was computed using the vif function in the package car of R, so as to evaluate multicollinearity (i.e. when different variables have a similar predictive relationship with the outcome). The vif function calculates the variance-inflation and generalized variance-inflation factors for linear, generalized linear, and other models. Any variable with a high VIF value (above 5) should be removed from the model.

A logistic model was fitted in order to identify the model that links the predicting variable Y, indicating rhodolith bed presence/absence, on the basis of the two predictors defined as the wave energy at the seabed and the bathymetry. Since the variable to predict is binary, the *binomial logistic regression* model was chosen.

The R function glm() was used, specifying the parameter family=binomial.

The fitted models were:

model1 < - glm(Y ~ X_1 + X_2, family = binomial(link = 'logit')) [1]

model2 < - glm(Y ~ X_1 * X_2, family = binomial(link = 'logit')) [2]

model3 < - glm(Y ~ X_1,family = binomial(link = 'logit')) [3]

model4 < - glm(Y ~ X_2, family = binomial(link = 'logit')) [4]

In [2], the operator * is used to test not only each single effect but also the interaction term between waves and bathymetry.

The Akaike Information Criteria (AIC) was used to identify the best model (e.g. the model characterised by both lowest index value and minimum number of parameters which still provides an adequate fit of data).

Despite the consideration of models with multiple predictors, the single predictors against Y = 1 were analysed separately in order to facilitate the model interpretation. Consequently, a plot for each predictor was produced. These identify the effect of each predictor against

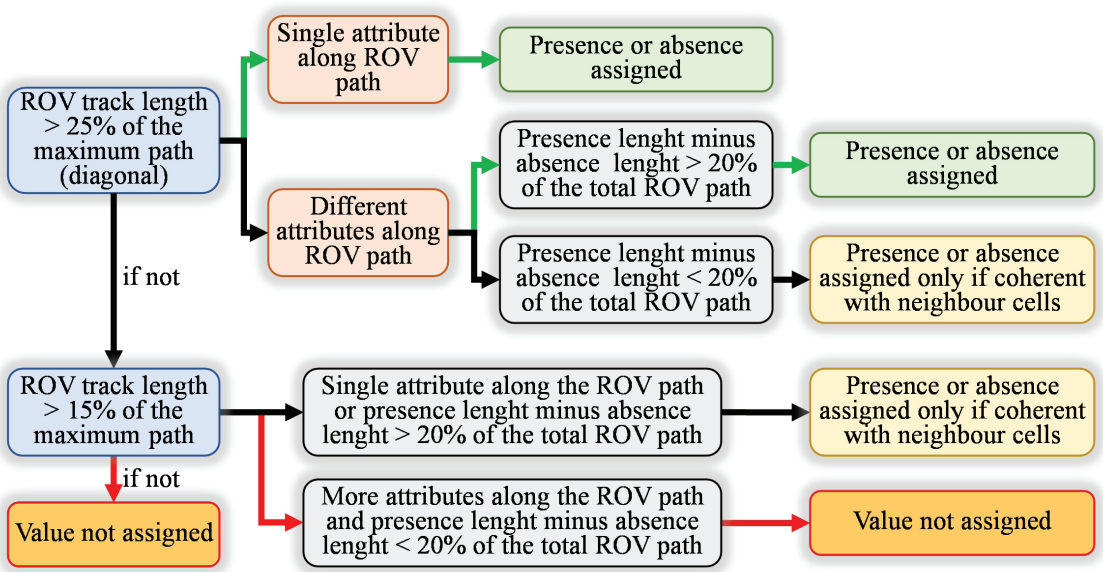

Fig. 3: Schema for designating rhodolith bed presence/absence attributes to the grid cells. Green arrows indicate the possibility to assign the presence/absence value, black arrows indicate needs of further step for the assignment while red arrows indicate that it is not possible to assign the presence/absence value.

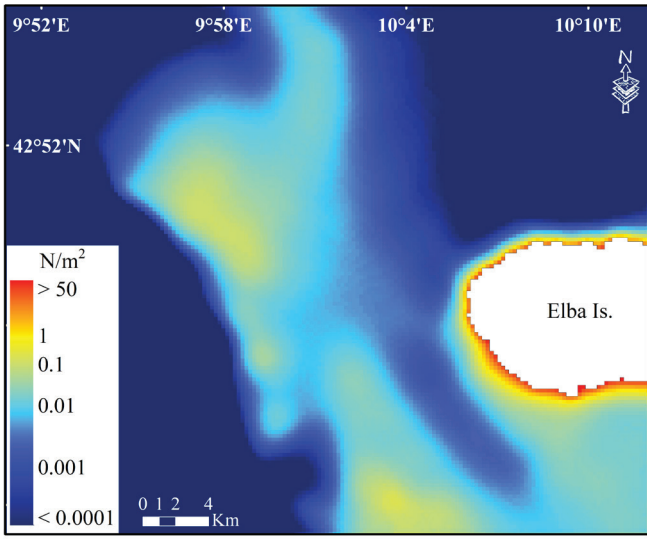

Fig. 4: 90-percentile of sea-bottom wave energy –target resolution (TR) domain.

the probability response = 1 of the dependent variable.

A linear discriminant analysis (LDA) was applied to classify absence and presence data based on the predictors. LDA is a classification method developed by Fisher (1936) based on a linear combination of predictors that best separates two classes. The R function lda() was used to perform the analysis while the partimat() function of the package (klaR) was used to visualize the results.

Results

The seabed energy map

Figure 4 describes the 90° percentile distribution map of wave energy at sea bottom at the target resolution (250 m). The circle indicates the area where most rhodoliths were observed. The sea bottom wave energy values highlight an area characterized by relatively high energy located in the north-west of the Elba Island. Although these energy values are approximately 1/100 of the maximum energy observed in the coastal zone, they would not be expected to occur at 50-60 meter depths.

Data analysis

Figure 5 consists of two different kernel density plots for the wave energy and bathymetry; the solid and the dotted lines represent respective rhodolith bed absence and presence.

The wave energy plot (Fig. 5A) illustrates that low energy values are characterised by overlapping rhodolith bed absence and presence lines, while higher energy values are characterized only by conditions of rhodolith bed presence.

The bathymetry plot (Fig. 5B) illustrates that the two presence/absence lines partially overlap only within a specific bathymetric range.

Binomial logistic regression model

The low VIF value (2.798444), estimated for model1, excludes the presence of multicollinearity allowing to also compare the nested models. Table 1 illustrates the results of the four Binomial logistic regression models.

In the first two models bathymetry is not statistically significant. The only statistically significant variable is the wave energy, which has the lowest p-value (model1) suggesting the association of wave energy with the probability of rhodolith bed occurrence. In model 2 the interaction between waves and bathymetry (X_1*X_2) is statistically significant, a condition which can be attributed to the wave energy influence on the sea bottom.

Models 3 and 4 provide insight on the influence of each variable separately against rhodolith bed presence. The higher p-value obtained when considering wave energy with respect to bathymetry confirms the significance of the former variable.

R anova() function on the models allows to analyse the table of deviance (Table 2). The three terms X_1, X_2, X_1*X_2 are added sequentially (first to last).

The difference between the null deviance and the residual deviance shows how the model performs against the null model (a model with only the intercept); the wider the gap, the better the model performance. Analysis of the results reported in the table indicates the drop in

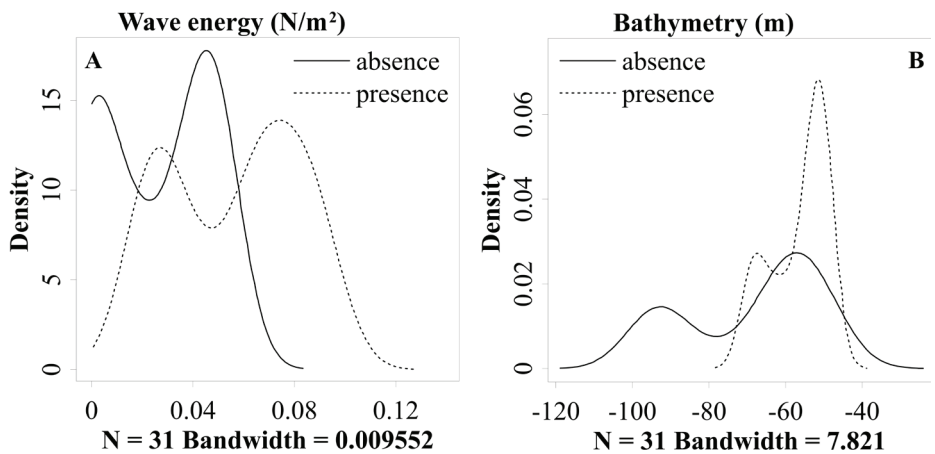

Fig. 5: Density plot: A) Wave energy (N/m²); B) Bathymetry (m).

Table 1. P-values associated at the coefficients of the four model fitting and relative AIC information.

	Intercept	X_1 (wave energy)	X_2 (bathymetry)	X_1*X_2	AIC
	P-value	P-value	P-value	P-value	
model1	0.9279	0.0576 .	0.6667		58.367
model2	0.3811	0.2519	0.9158	0.0617 .	81.665
model3	0.003484 **	0.000161 ***			56.556
model4	0.000474 ***		0.001164 **		60.762

Signif. codes: 0 '***' 0.001 '**' 0.01 '*' 0.05 '.' 0.1 ' ' 1

Table 2. Analysis of deviance table.

	Deviance	Resid. Deviance	Pr(>Chi)
NULL		100.631	
X_1	23.1250	77.506	1.518e-06 ***
X_2	0.0456	77.461	0.83092
X_1*X_2	3.7954	73.665	0.05139 .

deviance with each variable addition, the most noteworthy drop in residual deviance being that obtained with the addition; of wave energy. The introduction of the X_2 and X_1*X_2 terms does not appear to significantly improve the models since the large p-value associated to the models with these two variables explains the same amount of variation of the simpler X_1 model.

To plot each predictor separately, a separate model for each predictor (model3 and model4) was fit. This analysis allows to identify which variables should be entered as predictors.

The plots in Figure 6 describe the relationship between the probability of occurrence of rhodolith beds (Y=1) and each predictor variable. The relationship is positive in both cases; the probability increases with each predictor increase. In particular, the relationship is stronger for the wave energy, as the probability to find rhodolith bed increases as the wave energy increases. This fact is due to the clearer separation between absence and presence data (Fig. 6A). As showed by the black dots in the lower (absence) and upper (presence) part of the plot, the absence data are associated to lower wave energy values while presence data are associated to higher wave energy values. In the second plot (Fig. 6B) rhodolith bed presence is recorded at shallower depths whereas the absence values are spread throughout the entire bathymetric range thereby indicating that the relationship between the probability and this predictor is weaker.

The objective of the study was further pursued by identifying the variable value associated to the 0.8 probability of rhodolith bed occurrence observed using model3 and model4, i.e. using separately the wave energy and the bathymetry.

The value associated to the 0.8 probability of rhodolith bed occurrence was identified for each predictor together with the associated 97.5% confidence interval. These values are indicated in Figures 7A and 7B where the blue dots identify the respective predictor values and associated confidence intervals (blue lines).

The wave energy variable value associated to 0.8 rhodolith bed probability is 0.057 N/m^2 with an associated 97.5% confidence interval range of 0.042 N/m^2 - 0.072 N/m^2.

The bathymetry variable value for a 0.8 rhodolith bed probability is -52 m and its 97.5% confidence interval is between -60 and -46 m depth.

Classification using Linear Discriminant Analysis

The Linear Discriminant Analysis (LDA) is based on the concept of identifying a linear combination of predictors that best separates two (or more) classes.

The LDA applied to the present study indicates the

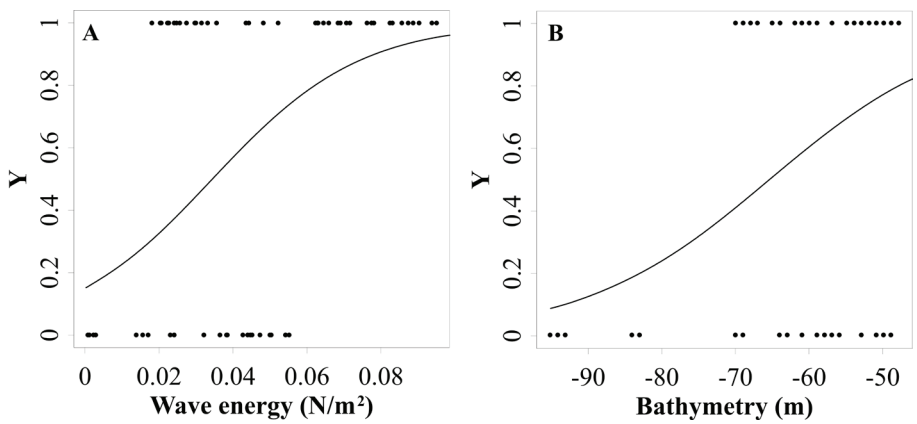

Fig. 6: Probability of finding rhodolith beds versus wave energy (A) and bathymetry (B).

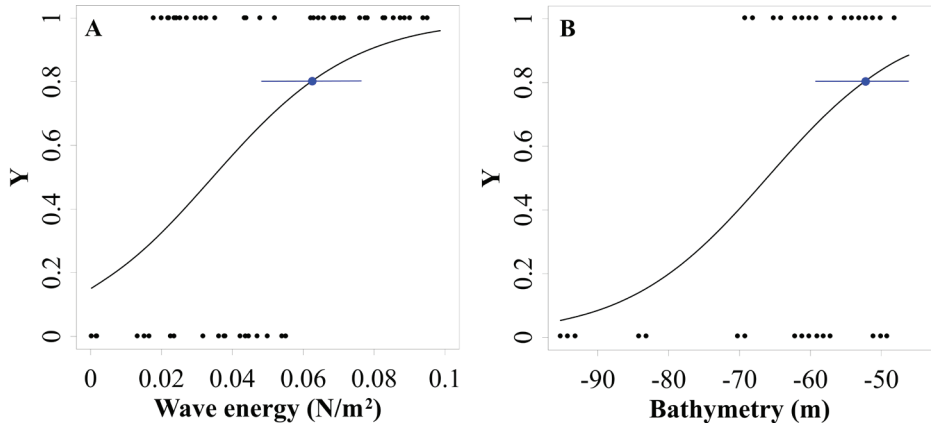

Fig. 7: Probability of rhodolith bed occurrence based on wave energy (A) and bathymetry (B) values.

linear combination of the two predictors (wave energy and bathymetry) that best separate the two observed classes of data: presence and absence of rhodolith beds.

The proportion of misallocated observations provides an estimate of the error rate.

Figure 8 shows the classification of the two groups, describing rhodolith bed presence (1) and absence (0), based on LDA methods. Misclassified observations are reported in red. Black bold dots are the centroids of the two groups. Moreover, the classification borders are displayed and the apparent error rate (0.392) is reported in the title.

The two groups (presence and absence) are characterized by different wave energy values summarised through the respective centroids, i.e. 0.057 N/m² for the presence group (light green area) and 0.024 N/m² for the absence group (light yellow area).

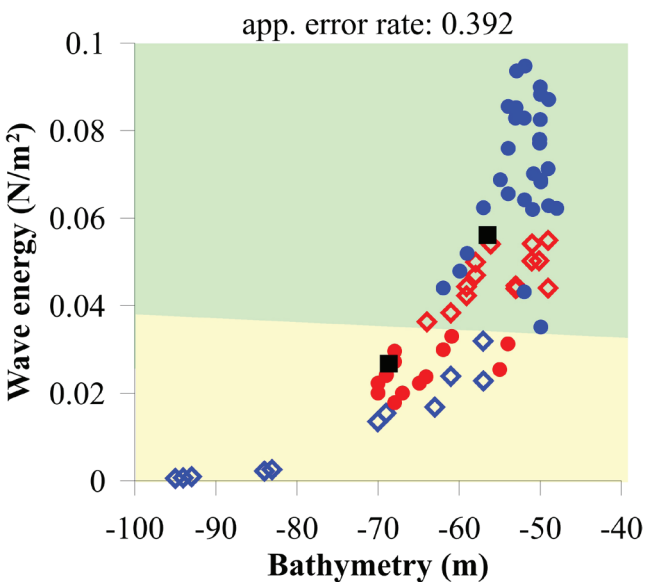

Fig. 8: LDA Classification of presence and absence of rhodolith beds. Rhodolith presence is reported using diamonds while absence is reported using circle. Blue symbols and red symbols indicate well-classified and misclassified records respectively. Furthermore, graph highlights the presence and absence domain by delimitating two sub zones: light yellow (absence) and light green (presence). Finally, black squares represent the presence/absence domain centroids.

Discussion

Rhodolith beds are amongst the seabed habitats of conservation value in the Mediterranean sea. They host a high degree of species and trophic group diversity (Barbera *et al.*, 2003) and, together with *Posidonia oceanica* seagrass beds and coralligenous formations, they are considered a protected benthic habitat object of specific EU fishery restriction measures (EU, 2019). Implementation of the fishing restriction and of other conservation related monitoring and assessment activities such as those dictated by the Habitat Directive (EU, 2013) and the Marine Strategy Framework Directive (EU, 2017), requires the availability of these habitats' spatial data. Protected habitat mapping initiatives, however, have mostly been centred in recent years on seagrass meadows (Centenera Ulecia, 2013) which have been object of longer standing conservation initiatives throughout the last decades. On the contrary, limited efforts have been conducted in modelling (Martin *et al.,* 2015) and describing the relationship between potentially significant enviromental variables and known rhodolith presence in the Mediterranean Sea (Basso *et al.,* 2017). While Martin *et al.,* 2015 suggest the overriding importance of some environmental variables (phosphate/silicate concentration and sea surface current) the broad scale resolution and the typology of the predictor variables considered by these authors do not allow a comparison with the results obtained in the high resolution in situ analysis described in the present study. In this context, efforts to develop a model capable of predicting rhodolith bed occurrence based on higher resolution predictor variables and *in situ* habitat data can help attain prompt policy implementation and conservation benefits.

The present case study tested and confirmed the importance of wave energy at the sea bottom as the driving abiotic variable capable of estimating the occurrence of rhodolith beds, in agreement with Joshi *et al.* (2017), in off-shore areas of the continental shelf. Since the estimate of the energy on the sea bottom is dependent on depth, the degree of correlation between wave energy and bathymetry with respect to rhodolith bed occurrence were considered separately in order to avoid that a dependence on the bathymetry could introduce a spurious dependence on wave energy. Although rhodolith bed occurrence is clear-

ly influenced by both variables, the probability of habitat occurrence is greater when considering wave energy thereby suggesting use of the associated energy values in habitat prediction models. This is further corroborated by the binomial logistic regression results which confirm the statistical significance of wave energy in describing rhodolith bed presence in the study area. The logistic model describing rhodolith bed presence based on wave energy indicates that energy value ranges between 0.04 and 0.07 N/m^2 provide a 0.8 probability of predicting rhodolith bed presence. The study results identify the wind-wave energy level range which can be used to assess potential habitat occurrence in the offshore continental shelf provided that adequate spatial resolution (250 m for the present study area) and very high resolution bathymetry and wind data are available. Considering that high resolution current data were not available for the study area and that currents are another important environmental variable influencing this habitat occurrence, it is also expected that the combined use of adequate resolution current data together with that of wind-waves could improve the rhodolith bed modelling confidence. Although the above listed energy value ranges cannot prove habitat presence in absolute terms, their use can lead to the identification of geographic areas potentially characterized by rhodolith beds thereby restricting the areas object of future *in situ* mapping initiatives while facilitating the attainment of policy protection objectives.

Acknowledgements

This study was carried out in the framework of the EMODnet Seabed habitats phase II (2013-2016) funded by the European Commission, DG Mare (EC contract no. MARE/2012/10) and it is partially based on the data collected by ISPRA within the project "Studio sulla presenza nelle acque italiane dei fondi a Maerl –Corallinacee libere, habitat di interesse conservazionistico" financed by the Italian Ministry of the Agricultural, Alimentary and Forest Politics in 2011 (ISPRA, 2014).

References

Agnesi, S., Annunziatellis A., Canese S., Giusti M., Salvati E. *et.al*., 2015. The importance of high resolution rhodolith bed maps in the protection of habitats of conservation value. p. 191-192 In: *Proceedings of the second Mediterranean Symposium on the conservation of Coralligenous and other Calcareous Bio-Concretions*, 29-30 October 2014, Portorož, Slovenia. Bouafif, C., Langar, H., Ouerghi, A. (Eds). RAC/SPA publ., Tunis.

Agnesi, S., Mo, G., Annunziatellis, A., Chaniotis, P., Korpinen, S. *et.al*., 2017. *Assessing Europe's Marine Protected Area networks – Proposed methodologies and scenarios*. Künitzer, A. (Ed). ETC/ICM Technical Report 2/2017, Magdeburg: European Topic Centre on inland, coastal and marine waters, 72 pp.

Al-Hamdani, Z., Reker, J., 2007. *Towards marine landscapes in the Baltic Sea ecoregion*. BALANCE Interim Report 10, 115 pp. http://balance-eu.org/xpdf/balance-interim-report-no-10.pdf.

Andersen, J.H., Manca, E., Agnesi, S., Al-Hamdani, Z., Lillis, H. *et.al*., 2018. European Broad-Scale Seabed Habitat Maps Support Implementation of Ecosystem-Based Management. *Open Journal of Ecology*, 8, 86-103.

Barbera, C., Bordehore, C., Borg, J.A., Glémarec, M., Grall, J. *et.al.,* 2003. Conservation and management of northeast Atlantic and Mediterranean maerl beds. *Aquatic Conservation: Marine and Freshwater Ecosystems*, 13, S65-S76.

Basso, D., Babbini, L., Ramos-Esplá, A. A., Salomidi, M., 2017. Mediterranean Rhodolith Beds. p. 281-298. In: *Rhodolith/Maërl Beds: A Global Perspective*. Riosmena-Rodríguez, R., Nelson, W., Aguirre, J. (Eds). Springer International publishing, Coastal Research Library 15, Switzerland.

Bianchi, C.N., Cinelli, F., Morri, C., 1996. La carta bionomica dei mari toscani: introduzione, criteri informativi e note esplicative. Atti della Società Toscana di Scienze Naturali, Memorie, ser. A, 102 Suppl. 1995, 255-270.

Birkett, D.A., Maggs, C.A., Dring, M.J., 1998. Maerl (Volume V). *An overview of dynamic, sensitivity characteristics for conservation management of marine SACs*. Scottish Association for Marine Science (UK Marine SACs Project). Natura 2000, v. 5, Peterborough. 116 pp.

Cameron, A., Askew, N., (Eds), 2011. *EUSeaMap - Preparatory Action for development and assessment of a European broad-scale seabed habitat map*. Final report. Available online at www.emodnet-seabedhabitats.eu/outputs.

Casaioli, M., Catini, F., Inghilesi, R., Lanucara, P., Malguzzi, P. *et.al*., 2014. An operational forecasting system for the meteorological and marine conditions in Mediterranean regional and coastal areas. *Advances in Science and Research,* 11, 11-23.

Centenera Ulecia, R., 2013. *Summary of the implementation of EU Regulation 1967/2006. Note*. Directorate General for Internal Policy Department B: Structural and Cohesion Policies – Fisheries.

Cogan, C. B., Todd, B. J., Lawton, P., Noji, T. T., 2009. The role of marine habitat mapping in ecosystem-based management. *ICES Journal of Marine Science*, 66, 2033-2042.

Connor, D.W., Gilliland, P.M., Golding, N., Robinson, P., Todd, D. *et.al*., 2006. *UKSeaMap: the mapping of seabed and water column features of UK seas*. Joint Nature Conservation Committee, Peterborough, 80 pp.

De Falco, G., De Muro, S., Batzella, T., Cucco, A., 2011. Carbonate sedimentation and hydrodynamic pattern on a modern temperate shelf: the strait of Bonifacio (western Mediterranean). *Estuarine, Coastal and Shelf Science*, 93, 14-26.

EU, 2013. Council Directive 92/43/EEC of 21 May 1992 on the Conservation of Natural Habitats and of Wild Fauna and Flora. *Official Journal of the European Union* L43, 1-56. https://eur-lex.europa.eu/eli/dir/1992/43/2013-07-01 (accessed 13/05/2020)

EU, 2017. Directive 2008/56/EC of the European Parliament and of the Council of 17 June 2008 establishing a framework for community action in the field of marine environmental policy (Marine Strategy Framework Directive). *Official Journal of the European Union* L56, 1-27. https://eur-lex.europa.eu/legal-content/EN/TXT/PDF/?uri=CEL-

EX:02008L0056-20170607&rid=1 (accessed 13/05/2020)

EU, 2019. Council Regulation (EC) No 1967/2006 of 21 December 2006 concerning management measures for the sustainable exploitation of fishery resources in the Mediterranean Sea, amending Regulation (EEC) No 2847/93 and repealing Regulation (EC) No 1626/94. *Official Journal of the European Union* R1967, 1-25. https://eur-lex.europa.eu/legal-content/EN/TXT/PDF/?uri=CELEX-:02006R1967-20190814&rid=1 (accessed 25/06/2020)

Fisher, R.A., 1936. The use of multiple measurements in taxonomic problems. *Annals of Eugenics*, 7, 179-188.

Galparsoro, I., Borja, A., Uyarra, M. C., 2014. Mapping ecosystem services provided by benthic habitats in the European North Atlantic Ocean. *Frontiers in Marine Science*, 1, 23.

Grant, W.D., Masden, O.S., 1986. The continental-shelf bottom boundary layer. *Annual Review of Fluid Mechanics*, 18, 265-305.

Harris, P.T., Tsuji, Y., Marshall, J.F., Davies, P.J., Honda, N. *et.al*., 1996. Sand and rhodolith-gravel entrainment on the mid-, outer-shelf under a western boundary current: Fraser Island continental shelf, eastern Australia. *Marine Geology*, 129, 313-330.

Harris, P.T., 2012. Surrogacy. p. 97-114. In: *Seafloor geomorphology as benthic habitat: GeoHab Atlas of Seafloor geomorphologic features and benthic habitats*. Harris, P.T., Baker, E.K. (Eds). Elsevier, Amsterdam

Inghilesi, R., Orasi, A., Catini, F., 2016. The ISPRA Mediterranean Coastal Wave Forecasting system: evaluation, perspectives. *Journal of Operational Oceanography*. 9, 89-98.

Hasselmann, K., Barnett, T., Bouws, E., Carlson, H., Cartwright, D. *et.al.,* 1973. Measurements of wind-wave growth and swell decay during the Joint North Sea Wave Project (JONSWAP). *Deutsche Hydrographische Zeitschrift* , Suppl. A, 8(12), 95 p.

ISPRA 2014. Studio sulla presenza nelle acque italiane dei fondi a Maerl- Corallinacee libere, habitat di interesse conservaizonistico. Relazione finale. Progetto di ricerca 7 A 18 CUP J85E11000770001. 66 pp. + annexes. (Public technical report available upon request).

Joshi, S., Duffy, G.P., Brown, C., 2017. Mobility of maerl-siliciclastic mixtures: impact of waves, currents and storm events. *Estuarine, Coastal and Shelf Science*. 189, 173-188.

Kantha, L., Clayson, C., 2000. Small scale processes in Geophysical Fluid flows. Academic Press, vol. 67, 750pp.

Komen, G. J., Cavaleri L., Donelan, M., Hasselmann, K., Hasselmann S. *et.al*., 1994. *Dynamics and modelling of ocean waves*. Cambridge University Press. 532pp.

Korpinen, S., Meidinger, M., Laamanen, M., 2013. Cumulative impacts on seabed habitats: an indicator for assessments of good environmental status. *Marine Pollution Bulletin*, 74 (1), 311-319.

Levin, N., Coll, M., Fraschetti, S., Gal, G., Giakoumi, S.*et al*., 2014. Biodiversity data requirements for systematic conservation planning in the Mediterranean Sea. *Marine Ecology Progress Series*. 5, 261-281.

Marrack, E.C., 1999. The relationship between water motion, living rhodolith beds in the southwestern Gulf of California, Mexico. *PALAIOS*. 14, 159-171.

Martin, C. S., M. Giannoulaki, F. De Leo, M. Scardi, M. Salomidi, L. *et al.,* 2015. Coralligenous and maërl habitats: predictive modelling to identify their spatial distributions across the Mediterranean Sea. *Scientific Reports* 4, 5073.

Michez, N., Fourt, M., Aish, A., Bellan, G., Bellan-Santini, D. *et.al.,* 2014. *Typologie des biocénoses benthiques de Méditerranée Version 2*. Rapport SPN 2014 - 33, MNHN, Paris, 26 pp.

Mitchell, A.J., Collins, K.C., 2004. Understanding the distribution of maerl, a calcareous seaweed, off Dorset, UK, pp. 65-82. In: *GIS/Spatial Analyses in Fishery, Aquatic Sciences (Vol. 2)*. Nishida, T., Kailola, P.J., Hollinworth, C.E. (Eds). Fishery-Aquatic GIS Research Group, Saitama, Japan. 735pp.

Pugh, D., Woodworth, P. 2014. *Sea-Level Science: Understanding Tides, Surges, Tsunamis and Mean Sea-Level Changes*. Cambridge: Cambridge University Press.

R Core Team, 2017. R: A language and environment for statistical computing. R Foundation for Statistical Computing, Vienna, Austria. URL https://www.R-project.org/.

Rattray, A., Ierodiaconou, D., Womersley, T., 2015. Wave exposure as a predictor of benthic habitat distribution on high energy temperate reefs. *Frontiers in Marine Science*, 2. 8pp.

Roff, J.C., Taylor, M.E., 2000. Viewpoint: national frameworks for marine conservation a hierarchical geophysical approach. *Aquatic Conservation: Marine and Freshwater Ecosystems*, 10, 209-223.

Roff, J.C., Taylor, M.E., Laughren, J., 2003. Geophysical approaches to the classification, delineation and monitoring of marine habitats and their communities. *Aquatic Conservation: Marine and Freshwater Ecosystems*, 13, 77–90.

Sañé, E., Chiocci, F.L., Basso, D., Martorelli, E., 2016. Environmental factors controlling the distribution of rhodoliths: An integrated study based on seafloor sampling, ROV and side scan sonar data, offshore the W-Pontine Archipelago. *Continental Shelf Research*, 129, 10-22.

Soulsby, R. L., 2006. Simplified calculation of wave orbital velocities, report TR 155, HR Wallingford.

Soulsby, R.L., 1997. Dynamics of Marine Sands. A Manual for Practical Applications, Thomas Telford Publications, Thomas Telford Services Ltd, London, 1997, 249pp.

Steller, D.L., Foster, M.S., 1995. Environmental factors influencing distribution, morphology of rhodoliths in Bahia Concepcion, B.C.S., Mexico. *Journal of Experimental Marine Biology*, Ecology 194, 201-212.

Templado, J., Capa, M., Guallar, T, J., luque, A., 2009. 1170 Arrecifes. En: VV.AA., Bases ecológicas preliminares para la conservación de los tipos de hábitat de interés comunitario en España. Madrid: Ministerio de Medio Ambiente, y Medio Rural y Marino. 142 pp.

Vasquez, M., Mata Chacón, D., Tempera, F., O'Keeffe, E. Galparsoro, I.,*et.al*., 2015. Broad-scale mapping of seafloor habitats in the north-east Atlantic using existing environmental data. *Journal of Sea Research*, 100, 120-132.